NASA TECHNICAL MEMORANDUM

NASA TM X-71737

NASA TM X-71737

SEPARATION OF THE STRAIN COMPONENTS FOR USE IN STRAINRANGE PARTITIONING

by S. S. Manson
Case-Western Reserve University
Cleveland, Ohio

and

G. R. Halford and A. J. Nachtigall
Lewis Research Center
Cleveland, Ohio

TECHNICAL PAPER to be presented at
Pressure Vessels and Piping Conference
sponsored by the American Society of Mechanical Engineers
San Francisco, California, June 23-27, 1975

N.C.P.

ABSTRACT

Two methods are presented for separating the inelastic strain components of a complex hysteresis loop so that Strain-range Partitioning formulas can be applied to accurately determine cyclic life at elevated temperatures. These methods are required only if lower bounds established by Strain-range Partitioning concepts have been deemed inadequate in the establishment of expected lifetime. In one method rapid loading and unloading is applied in the tensile and compressive half to isolate the plastic strain. In the second method the "creep" is measured at a discrete number of points along the hysteresis loop by combining load-control tests into the general pattern of strain cycling under arbitrary temperature. Both methods are shown to give good results.

SEPARATION OF THE STRAIN COMPONENTS FOR USE IN STRAINRANGE PARTITIONING

by

S. S. Manson, Case-Western Reserve University, Cleveland, Ohio

G. R. Halford, NASA Lewis Research Center, Cleveland, Ohio

A. J. Nachtigall, NASA Lewis Research Center, Cleveland, Ohio

SUMMARY

The basic principles of Strainrange Partitioning are reviewed, and two methods are presented for separating the inelastic strain components of the hysteresis loop for use in situations when a simple lower bound on life determinable from Strainrange Partitioning concepts is inadequate for design purposes. In one method of separation of the creep and plastic strain components, rapid loading and unloading is applied in the tensile and compressive halves of the cycle to isolate the plastic strain. In the second method, "creep" is measured at discrete points along the hysteresis loop by introducing load-controlled testing into the cycle so that the creep strains can be identified in association with periods of constant stress. Both methods are applied to a series of strain-controlled tests on 316 stainless steel at 1300 F (978 K) in which the rate of straining differs in the two directions of loading. Both methods are shown to result in predictions of lives that are within factors of 1.5 of the observed lives. It is shown also that the steady-state component of time-dependent strain is the most important "creep" component, and that the steady-state creep rate obeys a power-law relation to stress, relatively independent of loading history.

SEPARATION OF THE STRAIN COMPONENTS FOR USE IN STRAINRANGE PARTITIONING

by

S. S. Manson, Case-Western Reserve University, Cleveland, Ohio

G. R. Halford, NASA Lewis Research Center, Cleveland, Ohio

A. J. Nachtigall, NASA Lewis Research Center, Cleveland, Ohio

E-8366

INTRODUCTION

The concept of Strainrange Partitioning was introduced (1) four years ago at the First National Congress on Pressure Vessels and Piping. We proposed at that time that this method had the potential of treating complex creep-fatigue problems encountered in the components of interest to this assemblage. Several applications of the favorable use of this method were presented at that time, but the concept was too new to provide conclusive evidence of its direct utility. Since then, however, additional research (2,3) has convincingly placed the method as one of the foremost contenders among those capable of unifying this complex field.

One of its powerful advantages is that it permits treatment of problems involving arbitrary variation of strain and temperature as a function of time. Thus complex thermo-mechanical problems can be handled individually on the basis of true variation of service conditions, rather than requiring idealizations that may miss some of the essence of the problem.

One approach is to determine the lower bound of life based on the Strainrange Partitioning formulas. For example, a cycle may contain a tensile strain component which consists of only plastic flow, while the compressive component may be an unknown mixture of creep and plasticity. If the Strainrange Partitioning formulas indicate that for this material the most damaging combination would

result if all the compressive strain were creep, a conservative life estimate can be estimated directly from the basic data characterizing the material by assuming that all the compressive strain is creep, rather then by determining how much is creep and how much plasticity. For an application where the life so determined is acceptable, no further procedures are needed. If, however, the conservative life estimate is too low for design use it becomes necessary to determine a more accurate life estimate by detailed partitioning of the strains involved in the compressive half of the cycle. The basic strainrange components that underlie the partitioning concept can then be determined, and a suitable damage rule can then be applied to determine the life more precisely. In the more general case, both the tensile and the compressive halves of the cycle must be properly partitioned to determine the strainrange components. The partitioning procedure can be analytical or experimental. If an analytical stress and strain analysis has been made according to accurate constitutive equations, then the creep and plasticity components are automatically known; it is simply a matter of retrieving the proper terms as they appear in the solution. Since the accuracy of the existing constitutive equations and of procedures for inelastic analysis are now under intense investigation, the analytical approach to partitioning will be left for later study.

An alternative approach is to use an experimental procedure. Results from experimental investigations would not only provide information for the specific cycles studied, but could provide a rational basis for establishing constitutive equations applicable in general. This report will concern itself primarily with the experimental approach. It will be assumed here that the temperature and total strain history is known either by measurement or by

appropriate calculation. The stress history can then, of course, also be established by noting the loads required to subject a uniaxial specimen through the known temperature and strain history.[1] Thus it can be assumed that the actual hysteresis loop is available.

In earlier work (3) a procedure was indicated for a case involving relatively simple loading. The temperature and strain rate were maintained constant in a given hysteresis loop, but frequency (i.e. strain rate) was varied from test to test to generate a number of different hysteresis loops. It was found that under these conditions the strain components could be experimentally identified, and fatigue life predicted as a function of frequency. Under more generalized conditions involving changes of strain rate or temperature within a single cycle, the method as previously used is not directly applicable because it cannot distinguish conditons occurring in the compressive half of the cycle from these that occur in the tensile half. Alternate methods are, therefore, required.

The purpose of this report is to address the important question of separating the total inelastic strain of an arbitrary hysteresis loop into its generic strainrange componets, so that a damage rule can be applied to combine their effects and compute the fatigue life. Two experimental methods will be discussed.

The Half-Cycle Rapid Load-Unload Method. This method is a variant of the one used earlier to predict successfully the effect of freequency at constant temperature. However, while the earlier method involved only the rapid loading between the stress extremities of the hysteresis loop, the modified method divides the loop into two halves so that the loading-unloading aspects in both tension and

[1]We shall consider here only the case of uniaxial stress, leaving stress triaxiality to future investigation.

compression can be properly accounted for in the complex cycle.

The Step-Stress Method. Here the temperature and strain histories are accurately reproduced to simulate the operating hysteresis loop. Once a stable loop is established, the known stress history is repeated in steps rather than continuously. The plastic strain and creep strain associated with each step change of stress are then established, and the net plastic and creep strains for the loop are established. Two variants of this method are discussed.

Although the above methods will be described and briefly illustrated, it must be emphasized that their development is still in an exploratory stage. Many details must yet be worked out, and their relative merits must yet be established. Alternative methods must also be developed.

BASIC PRINCIPLES OF STRAINRANGE PARTITIONING

In order to describe the various partitioning processes, it is necessary to draw on several of the principles of the method that have already been discussed in previous publications (1-3). For convenience these will be briefly summarized here.

The Strainrange Partitioning Concept

The approach was introduced to describe the creep-fatigue interaction. Basically it assumes the existence of two different types of strain which, for convenience, are designated as "plasticity" and "creep". Although the application of the method does not depend on the physical nature of the two strains, it is convenient[2] to regard these strains as occurring in different regions of the volume of the body. For example, it is convenient to regard "plasticity" as the type of inelastic strain that develops when the metallographic

[2]As a framework for logic only; the approach does not depend on the physical mechanisms involved.

slip planes are displaced relative to each other, and "creep" as the type of inelastic strain that develops when grain boundaries slide relative to one another (although it is recognized that this type of motion is not the only type that can occur during creep). Once the "creep" and "plasticity" strains are identified as two distinct types, occurring in different regions of the body, it becomes possible to hypothesize a mechanism for the "creep-fatigue" interaction.

For example, suppose it is assumed that by some process it were possible to apply a tensile strain which consists entirely of the "creep" type caused by sliding of the grains relative to each other mainly along the grain boundaries, as schematically illustrated in Fig. 1(c) where the sliding takes place along GH to produce G'H'. Suppose, further, that upon reversal of the strain the conditions were changed so as to produce compression by slipping along the crystallographic slip planes, as for example in Fig. 1(d) where the reverse plasticity takes place along EF to produce E'F'. For equal tensile and compressive strain, the external dimensions of the volume of material under consideration are returned to their original values, and no net external strain develops. Internally, however, there has been a change: grain boundary sliding has occurred in one direction while crystallographic plane slip has occurred in the opposite direction. If the same cycle is now repeated, more grain boundary sliding occurs in the same direction as in the first cycle, and more crystallographic slip also occurs in the same direction as it did in the first cycle. In other words, each cycle causes ratcheting of both grain boundary sliding and crystallographic planes slipping. Eventually the capacity of the material to accomodate such strain is exhausted, and a crack develops.

While a "pure" strain reversal of the type just described is difficult to accomplish, both from a physical point of view (because material continuity cannot be accommodated by only grain boundary sliding, or by only crystallographic slip without some effect on the shape of the grain boundary), and experimentally (because it is difficult to realize test conditions in finite time ranges that will drive the material to such distinct modes of deformation), it is conceivable that such idealized deformation can be approached if the test conditions are properly chosen. Figure 2 shows, for example, one such possible test which can bring about such a strain cycle. From B to C a relatively low stress is imposed which is considerably less than the yield stress. Negligible plastic flow occurs. This stress is held for a long period of time, and "creep" occurs along CD. At this point the temperature is reduced to a value well below where creep occurs and a compressive stress is rapidly applied to produce an inelastic compressive strain along DEAB which just balances the tensile creep CD. Because of the low temperature and high strain rate, the compressive inelastic strain is very close to the idealized "plasticity" (if we hypothesize further that "creep" signifies grain-boundary sliding, and that "plasticity" signifies slip plane sliding). Such a strainrange is designated $\Delta\varepsilon_{cp}$, the first subscript designating the type of strain occurring in the tensile half of the cycle, the second relating to the compressive half; c referring to "creep" and p to "plasticity".

In a similar manner, it is, of course, possible to generate a type of strainrange, $\Delta\varepsilon_{pc}$, in which tensile plasticity is balanced by compressive creep. When both tensile and compressive strains are applied at temperatures below the creep range, or if both are applied at such high rate that there is no time for creep to take

place, the strain that develops is designated $\Delta\varepsilon_{pp}$. On the other hand, if the temperature is high, and the stress (or strain rate) low, only creep will be induced in both halves of the cycle; the strain induced becomes $\Delta\varepsilon_{cc}$. Figure 3 shows the hysteresis loops for the four generic types of strainranges.

While the types of cycles indicated in Fig. 3 show idealized conditions under which "pure" strainranges of the basic generic types are induced, the actual case is one in which two or three of these strainrange types occur within the same cycle. Figure 4 shows one such cycle. Here both the tensile and compressive stresses are rapidly raised to their maximum values so that no creep occurs during the loading changes ABC or DD'E. Inelastic strains BC' and D'E' are, therefore, plasticity. Each stress is held for a period to induce creep: CD (or C'D') in tension, EA (or E'B) in compression. Thus, although the tensile plasticity is greater than the compressive plasticity, the compressive creep is greater than the tensile creep. From the figure it is apparent that the cycle includes a reversed plasticity $\Delta\varepsilon_{pp}$ = D'E', a reversed creep $\Delta\varepsilon_{cc}$ = C'D', and an unbalanced strain component $\Delta\varepsilon_{pc}$ = BC'-D'E' or BE'-D'C'.

Figure 4 shows a special case wherein each of the strain components is readily identifiable. All loads are rapidly applied, so that during their application only plasticity, not creep, occurs. During constant stress holding only creep occurs, no plasticity. In the more general case, however, temperature changes and gradual stress changes cause both creep and plasticity to be induced concurrently throughout the cycle. The process of separating the induced strains into their creep and plasticity components may be more difficult, but assuming that this can be done (the procedure

being the subject of this report), it is apparent that even the most complex cycle can be visualized as consisting of four main quantities: tensile creep, tensile plasticity, compressive creep and compressive plasticity. These quantities can then be synthesized into the quantities $\Delta\varepsilon_{pp}$, $\Delta\varepsilon_{cc}$, $\Delta\varepsilon_{cp}$, and $\Delta\varepsilon_{pc}$. (Of course, in any singe cycle only one, not both, of the strain types $\Delta\varepsilon_{cp}$ and $\Delta\varepsilon_{pc}$ can exist, depending on whether there is an excess of creep or plasticity in each of the directions.) Thus, no matter how complex the cycle, it can be characterized by stating the attendant strainrange components $\Delta\varepsilon_{pp}$, $\Delta\varepsilon_{cc}$, or $\Delta\varepsilon_{cp}$ (or $\Delta\varepsilon_{pc}$). Once the components are known, the life can be determined by procedures to be discussed.

The concept underlying Strainrange Partitioning is, therefore, that the creep-fatigue interaction is basically related to the manner in which creep and plasticity strains reverse each other. In any one cycle, only three generic types of strain reversals are possible, and the most complex cycle can be characterized by the magnitudes of the three strainrange types present. How to establish life from a knowledge of the strainrange components will be discussed in the next two sections; how to determine the strainrange components is the main subject of this report, and will be treated later.

The Basic Life Relationships

For pure generic strainrange types, the life relationships follow the Manson-Coffin form. Thus

$$\begin{aligned} N_{pp} &= A_1(\Delta\varepsilon_{pp})^{\alpha_1} \\ N_{cp} &= A_2(\Delta\varepsilon_{cp})^{\alpha_2} \\ N_{pc} &= A_3(\Delta\varepsilon_{pc})^{\alpha_3} \\ N_{cc} &= A_4(\Delta\varepsilon_{cc})^{\alpha_4} \end{aligned} \qquad (1)$$

where the coefficients A_1 to A_4 and the exponents α_1 to α_4 are individualized for each material, and have been found to be relatively independent of temperature for materials in which the ductility (both tensile and creep) are relatively independent of temperature. These life relations should be experimentally determined individually for materials of technological importance. However, for materials not yet accurately characterized, it is possible to estimate the life relations from a knowledge of the tensile and creep ductilities.

As an illustrative example, and for later use in the calculations to be described, the life relations for 316 stainless steel determined at 1300F (978 K) are shown in Fig. 5. These relationships are valid over the relatively large temperature range from 1000 to 1600 F (811 to 1144 K).

The Cumulative Damage Relation

Equations (1), and the illustrative graphical relations for 316 stainless steel as shown in Fig. 5, are valid only when a single pure strainrange of the type indicated is present. When more than one type of strainrange is present, as in Fig. 4, a cumulative damage relation is required. The "Interaction Damage Rule", as discussed in Ref. (3), has been found satisfactory for this purpose. Let $\Delta\varepsilon_i$ be the inelastic strainrange of the hysteresis loop, and $\Delta\varepsilon_{pp}$, $\Delta\varepsilon_{cp}$, $\Delta\varepsilon_{pc}$ and $\Delta\varepsilon_{cc}$ be the corresponding generic strainrange components (of course, only $\Delta\varepsilon_{cp}$ or $\Delta\varepsilon_{pc}$ can exist, not both). Form the fractions

$$F_{pp} = \frac{\Delta\varepsilon_{pp}}{\Delta\varepsilon_i} \qquad F_{cp} = \frac{\Delta\varepsilon_{cp}}{\Delta\varepsilon_i}$$

$$F_{pc} = \frac{\Delta\varepsilon_{pc}}{\Delta\varepsilon_i} \qquad F_{cc} = \frac{\Delta\varepsilon_{cc}}{\Delta\varepsilon_i} \tag{2}$$

The interaction damage rule becomes

$$\frac{1}{N_f} = \frac{F_{pp}}{N_{pp}} + \frac{F_{cp}}{N_{cp}} + \frac{F_{pc}}{N_{pc}} + \frac{F_{cc}}{N_{cc}} \qquad (3)$$

Here N_{pp} is the life determined from Eq. (1) or Fig. 5 (for example), when the inelastic strainrange $\Delta\varepsilon_i$ is substituted into the PP relation. Similarly N_{cp}, N_{pc}, N_{cc} are the lives determined by using the corresponding life relations, again when the strainrange $\Delta\varepsilon_i$ is used in the appropriate relation.

For example, if the hysteresis loop were the one shown in Fig. 4,

$$F_{pp} = \frac{D'E'}{BD'} \ , \ F_{cc} = \frac{C'D'}{BD'} \ , \ F_{pc} = \frac{BC'-D'E'}{BD'} = \frac{BE'-D'C'}{BD'} \qquad (4)$$

The lives N_{pp}, N_{cc}, and N_{pc} are established by substituting the inelastic strainrange BD' successively into the life relations, Eq. (1).

SEVERAL PARTITIONING METHODS FOR COMPLEX CYCLES

In every type of hysteresis loop discussed thus far the type of strain induced during each increment of loading has been exclusively either "creep" or "plasticity", not both concurrently in a given time interval. Furthermore, it has been clear as to which type of strain was induced because the load was either very rapidly applied (resulting in "plasticity") or maintained constant at elevated temperature (resulting in "creep"). In the more general case, where the loading is more gradual, both types of strain may occur within the same time increment, and it becomes important to separate them so that a partitioning analysis can be made, and the interaction damage rule applied.

One approach for accomplishing the separation has already been described in Ref. (3) for the case of <u>continuous cycling at a constant frequency and temperature.</u> At very high frequency the inelastic strain is almost entirely of the $\Delta\varepsilon_{pp}$ type; at very low

frequencies it is almost entirely $\Delta\varepsilon_{cc}$. At intermediate frequencies both types of strain components occur. However, because of cyclic symmetry between the tensile and compressive halves of the hysteresis loop, neither of the unbalanced components $\Delta\varepsilon_{cp}$ or $\Delta\varepsilon_{pc}$ develop. The separation thus becomes simplified. The procedure will be briefly reviewed later. Here it is important to emphasize that the procedure cannot handle non-symmetrical loading resulting in the generation of either $\Delta\varepsilon_{pc}$ or $\Delta\varepsilon_{cp}$ strain. Other procedures are required. The main purpose of this report is to addresss the question of strainrange separation in the more general cases involving the existence of all of the generic types present.

To describe several procedures that are now under development we shall refer primarily to a specific application illustrated in Fig. 6. This application contains sufficient complexity to require a generalized approach applicable to other situations of even greater complexity; yet the complexity is minimized to permit ease of explanation and simplified experimental verification. As shown in Fig. 6(a), the main control variables are strain and strain rate. For simplicity, temperature is maintained constant, but well into the creep range of the material. It will be seen, however, that the methods described will permit treatment in similar manner of problems involving temperature changes during the cycle. The strain rate during loading along ABCD is also maintained constant at a value low enough to expect both "creep" and "plasticity" to occur concurrently. Unloading along DE is likewise at a constant strain rate, but at a much higher value than for loading. Although any unloading rate can be accomodated, it will be assumed for convenience that the rate is high enough essentially to exclude the development of "creep" strains. The material is caused to

cycle between a positive and negative strain of equal magnitude. The stress history is shown in Fig. 6(b), and the hysteresis loop in Fig. 6(c). Corresponding points in each of the three figures are clearly labeled.

Two different methods will now be discussed. Both are still in a stage of development, and questions regarding their application still need to be resolved. However, they are potentially useful, either in research in order to establish basic principles of material behavior, or for design and analysis of specific strain cycles. They have been successfully applied in several cases; but the description here will be limited to the loading cycle illustrated in Fig. 6. Results of other tests will also be cited later. The material tested was 316 stainless steel at 1300 F (978 K).

The Half-Cycle Rapid Load-Unload Method

In Ref. (3), a method was presented for separating the strain components in symmetrical cycles involving only $\Delta\varepsilon_{pp}$ and $\Delta\varepsilon_{cc}$ strains. Figure 7 shows the principle involved and the results obtained. Here the cycling was at a constant strain rate, both in tension and in compression, so that the plastic strain in tension was equal to that in compression. Thus, measuring the plastic strain over the complete cycle is adequate to determine how much occurs in tension as well as in compression. To measure the plastic flow over the entire cycle, it is only necessary to traverse the peak stresses rapidly. Thus, in Fig. 7 it is seen that at each frequency the continuous cycling hysteresis loop is first established (the wider of the hysteresis loops at A, B, C and D). Having once established the peak stresses, the cycling is changed to stress-control, and the peak stresses are traversed at a rate rapid enough to exclude creep. The thinner hysteresis loops at

A, B, C and D result. The width of the thinner hysteresis loop represents the plasticity strainrange $\Delta\varepsilon_{pp}$, while the creep strainrange $\Delta\varepsilon_{cc}$ is obtained by subtracting the plasticity from the width of the outer hysteresis loop which represents all of the inelastic strainrange. Note that the stress ranges developed are lower the lower the frequency. The "plasticity" loop is extremely thin at the low frequencies, but it comprises almost the entire width of the loop at the high frequencies. Thus, the inelastic strainrange is almost all $\Delta\varepsilon_{cc}$ at the low frequencies, and almost all $\Delta\varepsilon_{pp}$ at the high frequencies. Accordingly, fatigue life approaches N_{cc} at the lowest frequencies and N_{pp} at the highest frequencies. The S-shaped life curve of Fig. 7 shows good agreement with the predictions based on the interaction damage rule, Eq. (3), and the experimental results.

The procedure demonstrated in Fig. 7 is not directly applicable to the unsymmetric conditions of Fig. 6. It is not possible to traverse the complete stress range of the cycle, since the plasticity (and creep) of the tensile half differs from that of the compressive half. However, the same principle can be applied, treating each half cycle separately to determine its individual component of creep and plasticity. Figure 8 illustrates the procedure. The hysteresis loop ABCDEA is the same as that shown in Fig. 6; it is the stable loop for the conditions demonstrated in this figure. Once this stable loop is established, the specimen can be brought to point B and held briefly to adjust the equipment for test continuation at rapid strain rate from B to D', where D' is at the same stress as D. (A hold period at point B, where the stress is zero can readily be tolerated without seriously distorting subsequent response.) The rapid loading from B to D' produces no

creep, only plastic strain BE'. (The loading, in fact, need not be stopped at D'; it can continue on to any point F dictated by the limitations of the equipment.) Thus, for the tensile half of the hysteresis loop, we can assume that the plastic flow strain is BE' and the creep strain is E'E. The compressive half of the cycle may thus likewise be analyzed. Of course the loop should be re-stabilized before each rapid loading segment by traversing the cycle several times in real-time to obliterate the effects of the prior rapid-loading effects.

For the test shown in Fig. 6 the only quarter cycle where creep takes place is BD; in the more general case all four quarter cycles could conceivably involve creep strain. But the basic concept and procedure is clear for even the more general cases commonly encountered in service. Where temperature changes occur during the cycle, a question may arise as to what constant temperature to choose for the rapid loading period. In general the temperature should be that value at which the major plastic flow is expected to occur in the real-time cycle. Usually this will be the temperature that exists when the stress is in the vicinity of maximum value; however, cases involving rapid variations in temperature may require special consideration when using this method.

For the case of Fig. 8 it is clear that:

$$F_{pp} = \frac{BE'}{BE} \quad , \quad F_{cp} = \frac{E'E}{BE} \tag{5}$$

For more general cases the individual strainrange components can readily be identified by considering the net tensile and compressive plastic flow and creep strainranges. Some results obtained using this method will be presented later.

The Step-Stress Method

A further generalization of the above approach can be obtained

by increasing the number of steps from, and to, which the stress is rapidly changed. In Fig. 7 only one step is taken between the maximum and minimum stresses in the cycle; in Fig. 8 two step changes are taken, from zero to maximum and from zero to minimum. By increasing the number of steps the procedure can be generalized to treat any complex cycle involving arbitrary variation of stress, strain, and temperature. The step changes can involve the measurement of either plastic flow or creep. In the following discussion we shall describe the procedure for the approach involving creep measurements, and we shall illustrate experimental results obtained by this procedure. The more general case, involving plasticity measurements, - together with, or instead of, creep, - is described in Appendix A.

The method is illustrated in Fig. 9. Suppose that the hysteresis loop shown is the stable one obtained by several traversals of the real-time strain and temperature history. The problem resolves itself into determining experimentally the creep rates at a number of points along the loop, from which the overall creep can be determined. In Fig. 9(a) the stress levels E, A, B, C and D are chosen at the centers of the five intervals of equal strain into which the width of the hysteresis loop is arbitrarily divided. It is, of course, possible to choose the stress levels according to any scheme suitable for any particular problem.

In Fig. 9(a), the first step is to determine how much tensile creep occurs. The pertinent stress levels accordingly are, A, B, C and D which are above the strain axis. After the hysteresis loop has been stabilized, the first step, therefore, is to stop at point A and determine the creep rate, which can be done by holding the stress and temperature constant. (In order to accomplish suitable

stress-control, it may be advisable to momentarily relax the stress to zero or other appropriate value compatible with the equipment being used, while the strain-control mode is changed to stress-control. This is indicated by the dotted line AA". Afterwards, the stress is returned to A and held constant while creep occurs along AA'.) The creep deformation along AA' is shown in Figure 9(b) as a function of time. The time for which the stress A is held constant may be considerably longer than the time represented by interval 2 for which A is the central stress. The reason will become clear in the later discussion.

An important question arises as to how much of the time-dependent strain measured along AA' should be defined as "creep" for strainrange partitioning purposes. In the past we have regarded the "creep" strain, for purposes of strainrange partitioning, as all strain that is time-dependent, and "plasticity" as all strain that is time-independent. On this basis, all the strain shown in Fig. 9(b) would be regarded as "creep". Several prior unpublished NASA studies, together with the one under discussion, suggest that such definitions of "creep" and "plasticity" tend to attribute too much of the strain as belonging to the "creep" type. A closer re-examination of the principles underlying the concepts of strainrange partitioning also lead to the inference that not all the time-dependent strain should necessarily be assigned as "creep". The concept attributes, for example, the highly degrading influence of a $\Delta\varepsilon_{cp}$ type of strain to a ratcheting of two basically different types of strain, such as slip-plane sliding versus grain boundary sliding (used schematically here, not necessarily implying that these are the only two modes of deformation possible). Now it is very likely that even time-dependent strain can have components of both

types of strain. Conrad (Ref. 4) has, for example, cited cases for which the "creep" assignable to grain boundary sliding ranges between 2 to 30% of the total "creep". Thus we must really investigate very thoroughly which component of the time dependent strain is really "creep", and which components can be regarded as "plasticity" for strainrange partitioning purposes.

As a first approximation, it seems reasonable to assign all of the strain associated with the steady state creep rate as "creep", but to assume that only part, if any, of the transient strain is properly identified as "creep" for this purpose. Thus, we can assume

$$\delta_c = \delta_s + k\,\delta_{tc} \tag{6}$$

where

δ_c = effective creep

δ_s = steady state creep

δ_{tc} = transient creep

k = constant $(0 < k < 1)$

When $k = 0$ the transient creep is entirely neglected; when $k = 1$ it is entirely included. For purposes of convenient graphical solution it is desirable to determine an "effective creep rate" for the interval involved. When $k = 0$, the creep rate $\dot{\delta}_s$ is simply the slope of the linear creep curve in Fig. 9(b). If $k \neq 0$ the effective rate is determined by dividing the total creep of the interval according to Eq. (6) by the time of the interval. An illustration will later be discussed, and a tentative value suggested for k.

From the above discussion it is clear why the required time along AA' may exceed the real time of interval 2 represented by the stress at A: accurate establishment of the steady state creep rate in the interval may require extending the creep curve of Fig. 9(b)

beyond the interval time. No serious disadvantage accrues, however, in re-establishing points along the basic hysteresis loop because the loop is re-stablilized before proceeding to the next stress level B. Thus, for example, Fig. 10 shows the actual hysteresis loop for one of the tests to be discussed later. From A', the strain is returned to its negative extreme G, and in the very next cycle the basic hysteresis loop is precisely followed along AB. At B an analogous procedure is followed to determine the steady state creep rate, this time carrying the strain to B' well beyond the limit of the basic hysteresis loop GBEFG. In the first cycle of reload, the loop follows B'HGBE; but on the second reload GBEFG is re-established. Thus it is clear that re-stabilization of the hysteresis loop requires very few cycles, and that carrying out the test at any stress level to a time required to establish an accurate steady state creep does not interfere with the ability to determine creep properties under the real metallurgical structures associated with each selected point along the hysteresis loop. (Incidentally, the unloadings at A and B shown in Fig. 10 do not fall to zero stress because of the tare weight on the machine, but the change-over from strain-control to stress control was accomplished without influencing the return point on the hysteresis loop).

Once the effective creep rates have been established at the selected values of stress, a plot may be made as shown in Fig. 11 of the rates as a function of the time at which the rate is measured. Here stress becomes a dummy variable which establishes both the creep rate and the time within the cycle, but it does not actually enter directly into the plot itself. The area under the curve establishes the total tensile creep, as indicated in the figure. It is apparent that if only the steady-state time-dependent deformation is used as

the measure of "creep", a clearcut identification of "intervals" for the cycle is not even necessary; any set of judiciously selected stress levels within the loop establishes the curve and its associated area. If transient creep is included, an interval scheme is necessary according to Eq. (6), but the process is clearcut and simple.

Of course, if "creep" occurs in the compressive half of the cycle, a similar procedure is followed treating the creep associated with the compressive stresses in the same manner as described above for the tensile stresses. In Fig. 9(a), which reflects the loading pattern of Fig. 6, the only point in the compressive half of the loop where creep could occur is in interval 1. Very little creep was, however, measured in interval 1 because the high compressive stresses occurred for only a very short period of time (as was likewise the case for intervals 5 to 2 because of the rapid loading rate).

Once the "creep" components are established individually for the tensile and compressive halves, the plastic flow components can be obtained by subtraction from the total inelastic strain (the width of the loop), and the strainrange components computed according to the scheme analogous to Eqs. (4) and (5). The computed life is then obtained from Eq. (3).

While the above procedure emphasized the approach involving measurement of "creep", the more general approach may include or substitute plasticity measurements in each interval. The method, as already mentioned, is briefly described in Appendix A. It has not been studied in detail as yet, and will not be illustrated by actual test example in this report.

RESULTS AND DISCUSSION

Two different types of tests on 316 stainless steel will be

used to demonstrate the procedure and results for the partitioning methods described. In all cases the temperature was held constant at 1300 F (978 K) for convenience, although it will be recognized that at least for the step-stress method the basic approach would have been the same even if temperature variations would have occurred within the cycle. The first type of test is that illustrated in Fig. 6: the increasing strain ramping ($\dot{\varepsilon} > 0$) was slow and at a constant total strain rate; the decreasing strain ramping ($\dot{\varepsilon} < 0$) was rapid. Several increasing straining rates were used, but the decreasing strain ramping was as rapid as possible, being accomplished in approximately one second. In the second type of test the increasing strain ramping was rapidly applied in about one second, but the decreasing strain ramping was at the slow strain rate analogous to the slow ramping in the first type. For each of the two partitioning procedures a typical example will be illustrated in detail. Then the entire test program will be summarized and the procedures evaluated.

Example of the Half-Cycle Rapid Load-Unload Method

Figure 12 shows the details of the example wherein the test temperature was 1300 F (978 K), the total strain range approximately 1%, and the slow loading was applied at a total strain rate of .0072% s^{-1} (requiring 134 s to load), and the unloading was accomplished in about one second. The first step is to establish the stabilized hysteresis loop. Using closed-loop, servo-controlled, electro-hydraulic equipment, the hollow test specimens were strain-cycled according to the required pattern. (For details of test equipment and procedures, see Ref. (5). Within 20 cycles the hysteresis loop stabilized as shown by ABCDEA in the figure. The maximum stress determined at point D was 30 ksi (207 MN/m^2). The next step is to establish the plastic flow that occurs during the

tensile loading BCD. When point B is reached, therefore, the equipment is re-set for imposing the highest strain rate it can conveniently achieve, and the next loading is imposed this strain rate. As previously noted, it is not necessary to stop the loading precisely at the maximum stress developed in the stabilized loop; the loading can be extended to F if convenient. However, the intercept D' at the same stress as D is observed. Because of the rapid loading rate, the inelastic strain at D' is assumed to be all plasticity. Thus, from Fig. 12, in tension

ε_i = inelastic strain = 0.0065

ε_p = plastic strain = 0.0053

ε_c = creep strain = $\varepsilon_i - \varepsilon_p$ = 0.0012

In this case, since the compressive loading from E to A is at a very rapid rate, all the compressive inelastic strain is plasticity. Thus, of the 0.0065 compressive plastic flow, 0.0053 is used to balance tensile plastic flow, and 0.0012 is used to balance tensile creep. Then

$$\Delta\varepsilon_{pp} = 0.0053, \quad \Delta\varepsilon_{cp} = 0.0012$$

and

$$F_{pp} = \frac{\Delta\varepsilon_{pp}}{\Delta\varepsilon_i} = \frac{0.0053}{0.0065} = 0.815$$

$$F_{cp} = \frac{\Delta\varepsilon_{cp}}{\Delta\varepsilon_i} = \frac{0.0012}{0.0065} = 0.185$$

From Fig. 5, the life for a $\Delta\varepsilon_{pp}$ strainrange of 0.0065 is N_{pp} = 1160, and the life for an equal $\Delta\varepsilon_{cp}$ strainrange is N_{cp} = 76. Thus, using the Interaction Damage Rule Eq. (3)

$$\frac{1}{N_f} = \frac{0.815}{1160} + \frac{0.185}{76}$$

from which N_f = 319.

This value, together with others determined in a similar manner under different straining rates will later be compared to the

experimental life results.

Example of the Step-Stress Method

The same problem will now be treated by the step-stress method. As previously described, there are several procedures for using the step-stress method to determine the partitioned strain components. In one, the plastic component per interval is measured, and creep deduced by subtraction. Or, creep may be measured, and plasticity deduced. Or, both approaches may be taken and their results averaged. In this report we shall illustrate only the method involving the measurement of the creep component; the other methods although outlined in the Appendix are left to future study.

The first step, as before, is to obtain the experimental stabilized hysteresis loop by several traversals of the cycle in real time. This loop which has already been shown in Fig. 9 is thus the same as in Fig. 12 with the same test paramenters. Next the total strain of the cycle is divided into a convenient number of intervals. As shown in Fig. 9, five equal intervals have been used here, although a different number of intervals could be used, nor do they all have to represent equal strains. The creep rate at the center of each interval must then be determined.

Let us consider first the point A in Fig. 9 the center of interval 2 which is the first significant interval associated with the tensile loading. After several traversals of the hysteresis loop under strain control in real-time we may momentarily stop the loading at A. At this point the intent is to hold the stress constant in order to observe the pattern of creep behavior. In order to do so it is necessary to change to load-control. With our equipment, it is desirable to unload momentarily to point A" in order to effect the change-over without inducing spurious creep while

the change is being made. (This change requires approximately 10 seconds with our equipment.) Now the creep is observed along AA'. A direct tracing from the strain versus time record is shown in Fig. 13 at σ_A = 17.5 ksi (120 MN/m^2). Note that the creep is observed for a considerably longer time (7000 s) than that associated with interval 2 (27 s). It is held until a steady-state creep rate (linear plot on linear coordinates) is established.

After arriving at point A', it is now desirable to continue the cycling, and to establish the creep rate conditions at point B. However, because of the large creep time at the stress associated with A', the metallurgical state of the material has been somewhat altered. A new specimen could be used, of course, stopping for the first time at point B. But, fortunately, this is not necessary. It is well known that the metallurgical state can be restored in just a few traversals of the hysteresis loop in real-time. Typical results are shown in Fig. 10, as already discussed. Here it is seen that the loop restabilized after only one complete traversal. In dealing with test conditions that involve fatigue lives greater than approximately 50 cycles or so, the same specimen can be used for several re-stabilizations associated with the entire test; for test conditions involving very short lives, however, several specimens might be required. (But if the lives are short, predictions are not really necessary; a direct experimental life determination can be made.)

Having re-stabilized the loop, and arrived at point B the same procedure can be followed as at A, and a creep pattern observed as shown at σ_B = 25.0 ksi (173 MN/m^2) in Fig. 13. Similarly, points σ_C and σ_D can be so studied.

The next question to be answered is how to extract the proper

"creep" values from the curves shown in Fig. 13. As already discussed, use can be made of Eq. (6). In this example we shall first assume that only the steady-state deformation is active as "creep", that is k = 0. Afterwards we shall briefly examine another value chosen to improve the predictions.

On the basis that k = 0, the tensile "creep" for interval 2 is 0.000015, for 3 it is 0.000070, for interval 4 it is 0.000155, and for interval 5 it is 0.0003000. The steady state tensile creep for the tensile half is 0.00054. Applying the same approach to the compressive half of the cycle, it is apparent that the creep in intervals 5 to 2 is negligible because of the rapid loading rate involved. Compressive creep is possible in interval 1; however the actual time for which the high compressive stresses act is short, as seen in Fig. 6 and in fact the compressive creep is also negligible in this interval. Thus

$$F_{cp} = \frac{0.00054}{0.0065} = 0.083 \qquad F_{pp} = 1 - 0.083 = 0.917$$

Before applying the above strainrange fractions to calculate life, it is necessary to make several comments regarding the baseline fatigue life values with which they are to be combined in the Interaction Damage Rule. The baseline life values are shown in Fig. 5. However, it must be recognized that the basis upon which they were generated is different from that in which they are to be applied here. In generating the basic data <u>all</u> the time-dependent strain was regarded as creep, not only the component associated with the steady state creep rate. Of course the tests chosen to generate the baseline data did involve long hold-times at constant stress; thus a large fraction was, indeed, strain associated with steady state creep deformation. Some of it was, however, due to transient creep deformation. A re-examination of the strip-chart recordings

in connection with the generation of the baseline data suggests that 60 to 95% of the creep strain involved was steady state, the remainder of 5% to 40% was transient. At an inelastic strain range of 0.0065, approximately 70% of this creep strain was steady state. Recognizing the basic manner in which the numerics of the Interaction Damage Rule produce a value of fatigue life to be plotted in Fig. 5, it becomes clear that if only 70% of the creep strain had been used, the indicated value of N_{cp} for a given test condition featuring $\Delta\varepsilon_{cp}$ strain would become approximately 70% of what it was previously computed to be. Thus, as a first approach, to be consistent with the new concept of using only steady-state creep for the "creep" component, we must take values for N_{cp} and N_{pp} as follows:

$$N_{cp} = 53 \text{ cycles} \qquad N_{pp} = 1160 \text{ cycles}$$

Now applying the Interaction Damage Rule

$$\frac{1}{N_f} = \frac{0.917}{1160} + \frac{0.083}{53} ; \qquad N_f = 424 \text{ cycles}$$

This value of computed N_f, together with other values obtained at other test conditions, will later be compared to the experimental life values obtained under the conditions for which partitioning evaluations were made.

Test Results and Comparison with Experimental Fatigue Lives

Figure 14 shows the life predictions and test results associated with the half-cycle rapid load-unload method. The small closed circles show the predictions according to the procedure of Fig. 11 and associated discussion. Two S-shaped curves result. For the tests in which the slow ramping is for strain increases the predicted lives are very sensitive to the strain rate at which the tensile deformation is applied. At the low strain rates the life approaches the N_{cp} value, and at the high strain rates life approaches

the N_{pp} value. Since for 316 stainless steel the N_{cp} life is considerably lower than the N_{pp} life, a large variation in predicted life is indicated as strain rate is varied. Since all tests were not conducted at precisely the same strain level, the ordinate values are normalized relative to the N_{pp} life of the inelastic strain associated with each test in order to provide a viable single curve through all the predicted points. A few test points of actually measured fatigue lives are also shown along the curve. They lie relatively close to the curve of predicted life.

In the upper curve of Fig. 14 are shown the predictions and experimental results for the case analogous to Fig. 6, but in which the ramping increases of strain was rapidly applied (approx. one second), but the decreasing strain ramping was applied at a much slower rate. The major type of creep strain induced in this type of loading is $\Delta\varepsilon_{pc}$. Since for 316 stainless steel the N_{pc} life is considerably closer to the N_{pp} value than is the N_{cp} value for the same inelastic strainrange, the upper curve is relatively insensitive to straining rate compared to the lower curve. Again the predictions lie close to the experimental points.

Figure 15 shows the corresponding plot for the step-stress method. Again the two curves are S-shaped, and the experimental data points lie reasonably close to the predicted values. By assuming that $k = 0.1$ in Eq. (6) the experimental points could be made to coincide almost perfectly with the predictions for this case. Thus, for this problem, the indication is that the most appropriate assumption is that "creep" is the sum of the steady-state creep plus 10% of the transient creep. Considerable additional data are required, however, to generalize the behavior for other materials and test conditions.

A summary of all the tests is shown in Fig. 16. The experimental fatigue lives are plotted against the predicted values. Very good agreement is seen for either method.

Although both methods yield good results for this problem, it is recognized that each has its strengths and limitations. The half-cycle rapid load-unload method is easy to apply and yields results quickly with relatively little experimentation. It is ideally suited for a problem such as treated here in which the temperature is constant, since no ambiguity exists as to the temperature to be maintained during the rapid loading period. When temperature varies, it seems proper to use that temperature at which the maximum plastic deformation is likely to take place. Usually this is the temperature near the apex of the hysteresis loop where the stress is near maximum. However, the subject needs further study. The step-stress method is perfectly general, and lends itself to applications involving arbitrary variations of temperature and strain rate within the cycle. More effort is required to implement it, since strain rate determinations are required at a number of points, and since it is desirable (although not absolutely necessary) to stabilize the hysteresis loop between determinations. Its special value is that it involves measurements at true conditions of metallurgical structure at each pertinent point in the hysteresis loop, since the restabilization is expected to bring the material back essentially to its true structure. Not only is higher accuracy expected, therefore, but the technique permits generalized studies of material behavior as affected by the cycling process. Thus, through such generalized tests, better constitutive equations may evolve, and better simplified relations may be discovered for use in both experimental and analytical

partitioning processes.

Steady-State Strain Rate as a Function of Stresss

If the concept introduced in this report that for Strainrange Partitioning purposes the steady state creep component is of great importance in establishing "creep" turns out to have general validity, it would become very advantageous to provide a method for estimating the steady state creep rate. It would appear that, at a given temperature, the major parameter governing the creep rate is the instantaneous value of stress. A few tests on 316 stainless steel conducted in connection with the program being reported here have shown that while the rate of total creep is very sensitive to prior history and to the state of loading (e.g. loading versus unloading), the rate of steady state creep is less sensitive to these factors. The primary controlling factor is instantaneous stress. The results are shown in Fig. 17. Here steady-state creep rates, as determined through step-stress tests, are plotted against stress. Different symbols are used for the tests involving slow ramp increases of strain and those involving slow ramp decreases of strain. The points fall very nearly on a single curve. In fact, also shown in Fig. 17 are the results of some supplementary tests involving slow ramp straining for both increasing and decreasing strain. (In other words, continuous triangular straining from tension to compression to tension). Again the points fall reasonably close to those involving ramping in one direction only. Of course, this subject must be studied in greater detail. But if the results of Fig. 17 turn out to be general, the partitioning process will become greatly simplified. It may then be possible to represent the steady state creep rate by a simple power law of stress (modified, of course by a term that accounts for temperature). Both analytical

partitioning (through the constitutive equations which would also reflect this power law relation), and the experimental approach (which would now require fewer points of measurement), would benefit from this relation. Further pursuit of this subject is warranted for other loading conditions, temperatures, and materials.

CONCLUSIONS AND CONCLUDING REMARKS

In this report we have outlined two basic procedures for partitioning a given hysteresis loop. The first determines the plastic flow in the tensile and compressive halves respectively by rapid loading and unloading to the extreme stresses of the half-cycles; the "creep" deformation is determined by the difference from the known total inelastic strain. The second divides the cycle time into a number of intervals and seeks to establish either the plastic flow or the creep, or both values, within each interval. Although a generalized approach is described, the application presented is limited to the case in which only the "creep" is measured. This is accomplished by successive stress hold-periods at various points of the hysteresis loop. For the 316 stainless steel at 1300 F (978 K) tested during the experimental phase of the program, it was determined that the component of time-dependent deformation suitable for identification as "creep" for purposes of strainrange partitioning could be regarded with adequacy as that strain associated with the steady-state linear deformation. A small improvement could be obtained if it was assumed that 10% of the transient strain was also regarded as "creep", but the data were inadequate to generalize such an assumption.

The creep rate was found to obey approximately a power-law relation with stress, relatively insensitive to prior history or the nature of the complete history of loading within the cycle.

Very good results were obtained when the life predictions were made according to the two partitioning methods described. The types of loading examined consisted of ramped increasing strain at several strain rates with rapid strain decreases, and rapid strain increases followed by ramped decreasing strain at several strain rates. Further studies involving other materials and temperature and loading patterns are suggested for more complete verification of the methods.

The availability of a general method for separating the inelastic strain components brings the strainrange partitioning method an important step closer toward practical applicability as a design and analysis tool. Observation that the important "creep" component, (that associated with steady state creep), is governed by a power-law relation to stress, and that it is relatively insensitive to metallurgical structure influenced by prior loading history, may provide an extremely useful relation for analytical partitioning. This opportunity should be explored further.

REFERENCES

1 Manson, S. S., Halford, G. R., and Hirschberg, M. H., "Creep-Fatigue Analysis by Strainrange Partitioning," Design for Elevated Temperature Environment, ASME, 1971, pp. 12-24, DISC, pp. 25-28.

2 Halford, G. R., Hirschberg, M. H., and Manson, S. S. "Temperature Effects on the Strainrange Partitioning Approach for Creep-Fatigue Analysis," Fatigue at Elevated Temperatures, ASTM STP 520, American Society for Testing and Materials, 1973, pp. 658-667, DISC, pp. 668-669.

3 Manson, S. S. "The Challange to Unify Treatment of High Temperature Fatigue - A Partisan Proposal Based on Strainrange Partitioning," Fatigue at Elevated Temperatures, ASTM STP 520, American Society for Testing and Materials, 1973, pp. 744-775, DISC, pp. 775-782.

4 Conrad, Hans. "The Role of Grain Boundaries in Creep and Stress Rupture", Mechanical Behavior of Materials at Elevated Temperatures", John E. Dorn, Editor. McGraw-Hill Book Co., 1961.

5 Hirschberg, M. H. "A Low Cycle Fatigue Testing Facility," Manual on Low Cycle Fatigue Testing STP 465, American Society for Testing and Materials, 1969, pp. 67-86.

APPENDIX - GENERALIZATION OF THE STEP-STRESS METHOD

Rather than measuring the creep component of inelastic strain in each loading increment, the procedure can involve measurement of the plasticity component. Or both creep and plasticity can be measured. Figure 18 shows the procedure. The cycle is divided into a number of intervals, 10 for convenience here. For each interval the total inelastic strain is known from the hysteresis loop. The plastic strain can be determined from a rapid step change of stress representative of the stress variation within the interval; the creep can be measured by observing how much time-dependent strain occurs if the stress is held constant at a value characteristic of that interval (and at a temperature characteristic of that interval). Several variants of this procedure are possible, as will now be outlined. They are based on measurements of plastic strain and deduction of creep strain, measurement of creep strain and deductions of plastic strain, or measurements of both plastic and creep strains.

The determination of inelastic strain in any interval can be made directly from the stabilized hysteresis loop. In the interval 5, for instance, in Fig. 18(a), the elastic strain induced from B to C can be obtained by constructing through B a line of slope equal to the elastic modulus, and observing the intercept of a horizontal line through C. Thus, the inelastic strain in the interval is C'C. For future use it is designated δ_i.

To obtain the plastic flow in interval 5 it is merely necessary to change the rate of loading at point B to a value high enough to preclude significant creep. Thus BC" is the stress-strain relation obtained by loading as rapidly as possible after point B is reached. The measured plastic strain will be designated δ_p (C'C"). Whether or not this procedure is used to obtain plastic strain will depend

on the availability of equipment to accomplish this type of loading. Note, however, that the equipment need not be capable of stopping short at point C", a reasonable amount of overrun can be accomodated, but the point C" at a stress equal to that at C can be determined. Note further that this procedure can be followed for every desired interval, each point along the hysteresis loop being reached after several traversals of the complete hysteresis loop to stabilize it. Thus, every measurement is made more or less independent of the perturbations introduced in the material by prior loadings that caused the stress-strain behavior to deviate from the hysteresis loop.

From the known inelastic strain and plastic strain, the creep strain can be determined by subtraction. As noted in Fig. 18(a) the deduced value of creep strain in interval 5 is C"C. However, it is also possible to measure the creep strain directly. Such a procedure is desirable either as an independent approach, or in combination with the plastic strain measurement as already described in the body of this report.

Figure 19 shows how the data obtained in conjunction with the tests shown in Fig. 18 are synthesized and analyzed. In Fig. 19(a) are shown the basic measurements δ_i, δ_p, and δ_c. Each point is plotted at the center of the interval for which it was obtained While it is not necessary that all the quantities δ_p, δ_c, and δ_i be measured in order to provide an analysis (if two are measured the third can be determined by subtraction) it will be assumed in the following discussion that all are actually measured. Analyses based on more limited measurements have already been discussed.

Figure 19(b) shows that when all the measurements are made they are averaged to increase probable accuracy. Note that if δ_p and δ_i are measured, the creep strain can be determined as $\delta_i - \delta_p$.

However, if it is also measured as δ_c, the average value becomes $(\delta_i+\delta_c-\delta_p)/2$. Similarly, the average plastic strain for the interval becomes $(\delta_i+\delta_p-\delta_c)/2$. These synthesized quantities from Fig. 19(a) are thus plotted in Fig. 19(c). Since the total creep strain of the half cycle is the sum of the creep strains of all the associated intervals, the area under the $\bar{\delta}_c$ curve is a measure of ε_c, the creep strain of the half cycle. Similarly the area under the $\bar{\delta}_p$ curve is a measure of the plastic strain for the half cycle. Once the creep and plastic strains have been determined for the two half cycles, the partitioned strainrange components can be simply determined by methods analogous to Fig. 4 wherein it becomes clear how the tensile and compressive creep and plasticity components must combine to obtain $\Delta\varepsilon_{pp}$, $\Delta\varepsilon_{cc}$, and $\Delta\varepsilon_{pc}$ (or $\Delta\varepsilon_{cp}$).

While the procedure described above involves returning the material to the stabilized state prior to each step measurement, it is, of course, possible to reduce the test time by combining some of the steps and minimizing the re-stabilization. For example, in Fig. 18(a), once the material has been brought to point C" by a step change in stress, the stress could be held steady and the material allowed to creep for the time increment associated with interval 5. Presumably the creep would move the material to point C if the behavior were exactly as hypothesized. At this point the rapid step change in stress to a value equal to the stress at point D could be instituted, and the process repeated. As long as the material follows the stabilized hysteresis loop with reasonable proximity, this approach could be satisfactory. But if deviations from the basic hysteresis loop build up, it is probably best to traverse the complete hysteresis loop several times in order to restabilize it, and develop the analysis of another large segment

of the loop by starting again from another point upon it. Optimization of the procedure requires further study.

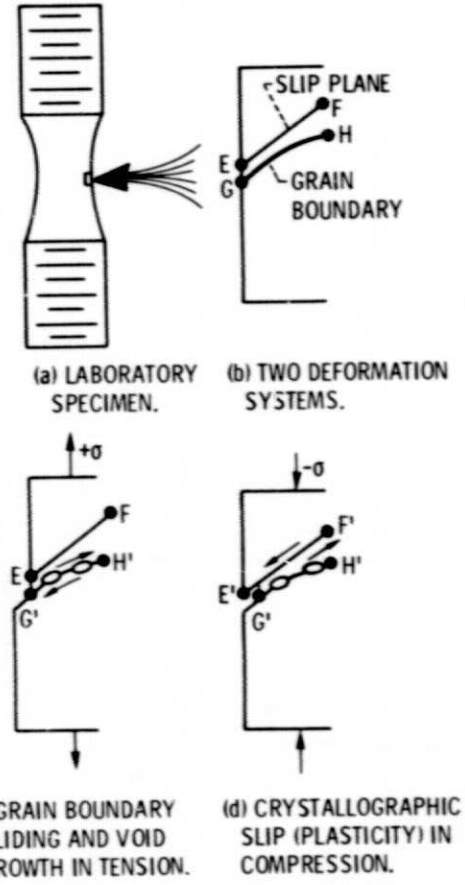

(a) LABORATORY SPECIMEN.

(b) TWO DEFORMATION SYSTEMS.

(c) GRAIN BOUNDARY SLIDING AND VOID GROWTH IN TENSION.

(d) CRYSTALLOGRAPHIC SLIP (PLASTICITY) IN COMPRESSION.

Figure 1. - Simplified schematic illustration of the creep-fatigue interaction occurring when tensile creep occurring along grain boundaries is reversed by compressive plasticity occurring along crystallographic slip planes.

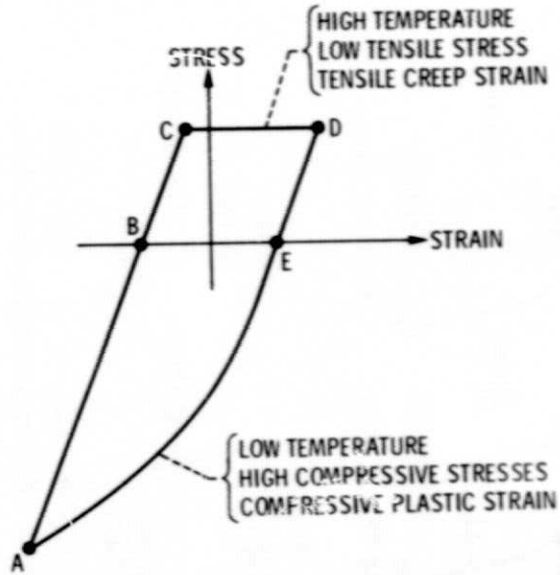

Figure 2. - Loading history conducive to tensile creep balanced by compressive plasticity.

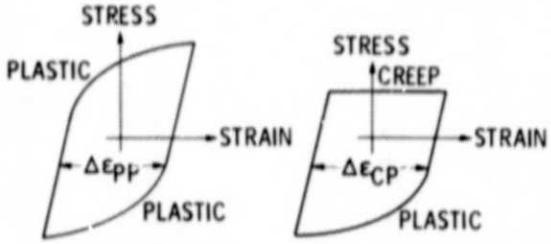

(a) PP TYPE CYCLE. (b) CP TYPE CYCLE.

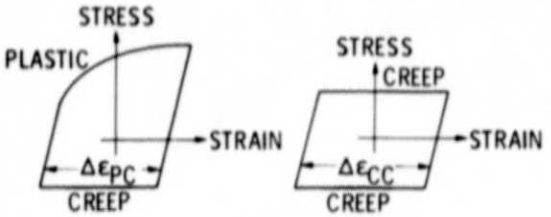

(c) PC TYPE CYCLE. (d) CC TYPE CYCLE.

Figure 3. - The four generic types of strainranges.

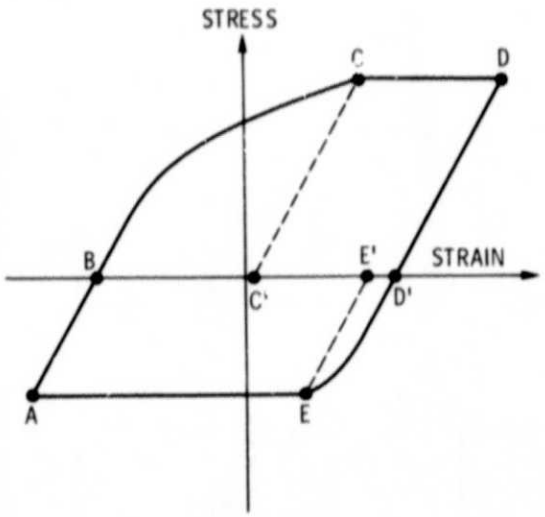

$\Delta\varepsilon_{PP}$ = D'E'

$\Delta\varepsilon_{CC}$ = C'D'

$\Delta\varepsilon_{PC}$ = BC' - D'E' = BE' - D'C'

Figure 4. - Hysteresis loop involving $\Delta\varepsilon_{PP}$, $\Delta\varepsilon_{CC}$, and $\Delta\varepsilon_{PC}$.

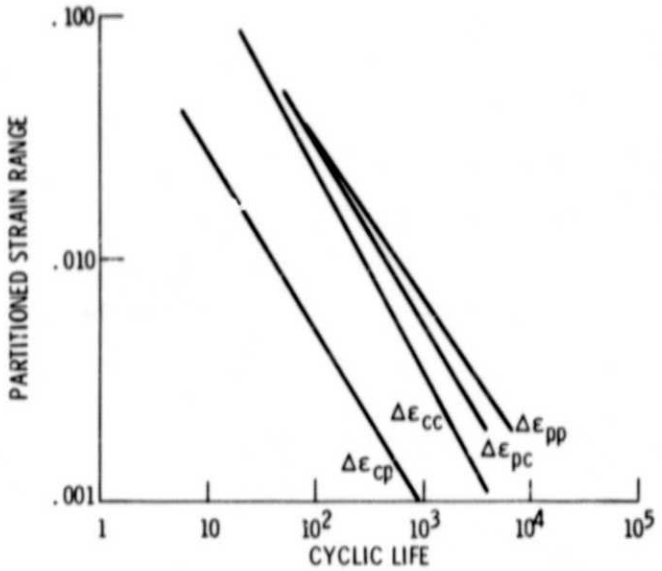

Figure 5. - Life relationships for generic strainrange components for 316 stainless steel at 1300° F (978 K).

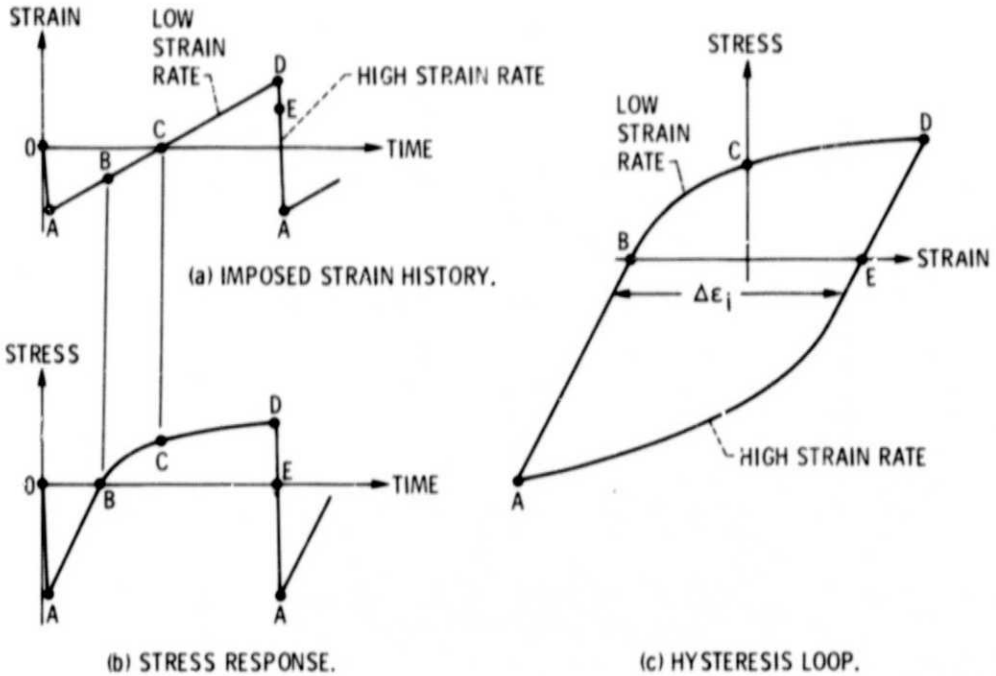

Figure 6. - Schematic illustration of hysteresis loop developed under unsymmetrical straining rates in tension and compression.

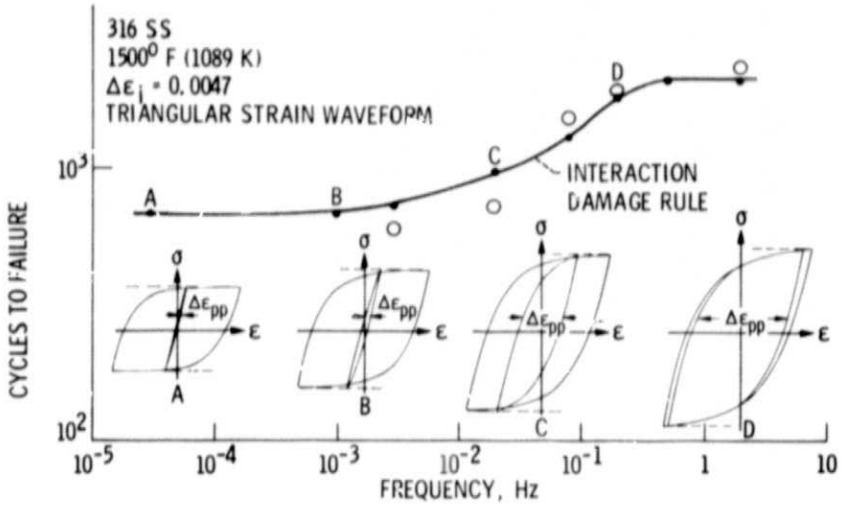

Figure 7. - Method of partitioning using real-time hysteresis loop and rapid-cycling hysteresis loop between same stress peaks. (Ref. 3).

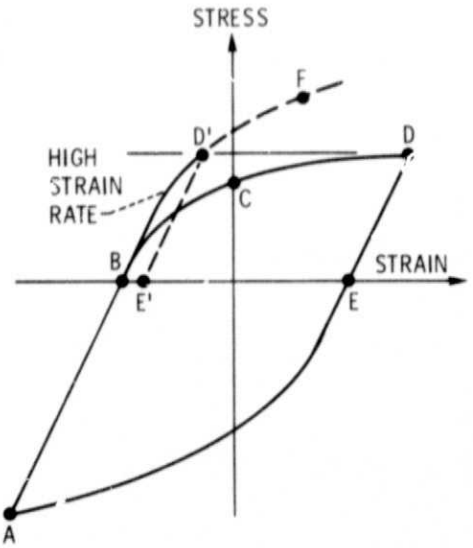

Figure 8. - Application of the half-cycle rapid load-unload method for partitioning.

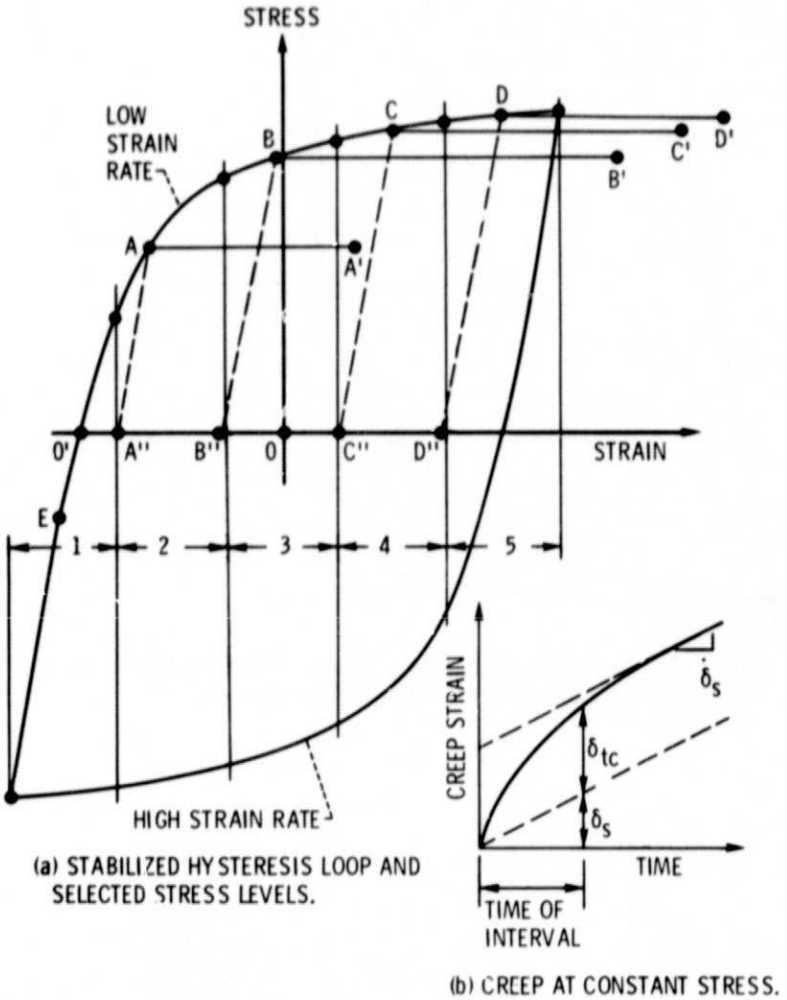

(a) STABILIZED HYSTERESIS LOOP AND SELECTED STRESS LEVELS.

(b) CREEP AT CONSTANT STRESS.

Figure 9. - Selection of several stress levels along the hysteresis loop where stress-hold tests are conducted to determine creep rates.

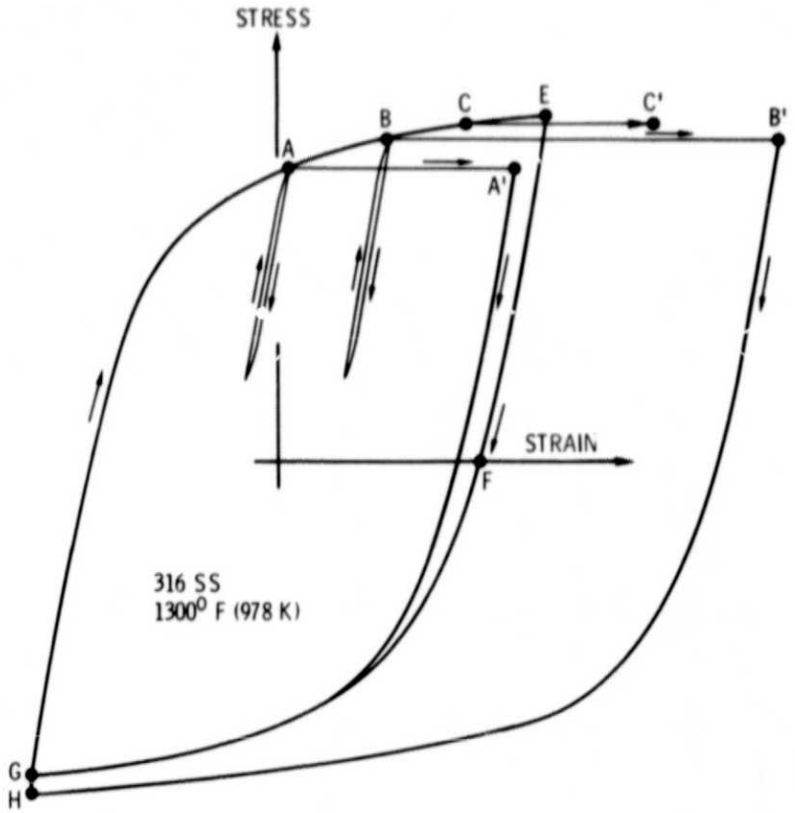

Figure 10. - Actual hysteresis loops for re-loadings after steady-state creep rates have been established at various points in the cycle.

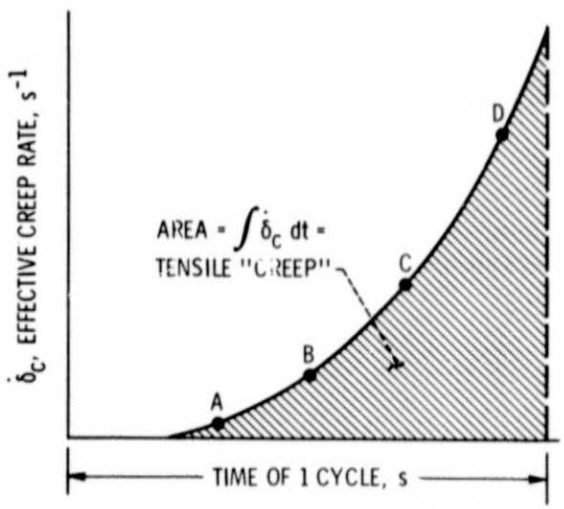

Figure 11. - Determination of "creep" as area under the plot of creep rate versus time at points in cycle where creep rate is measured.

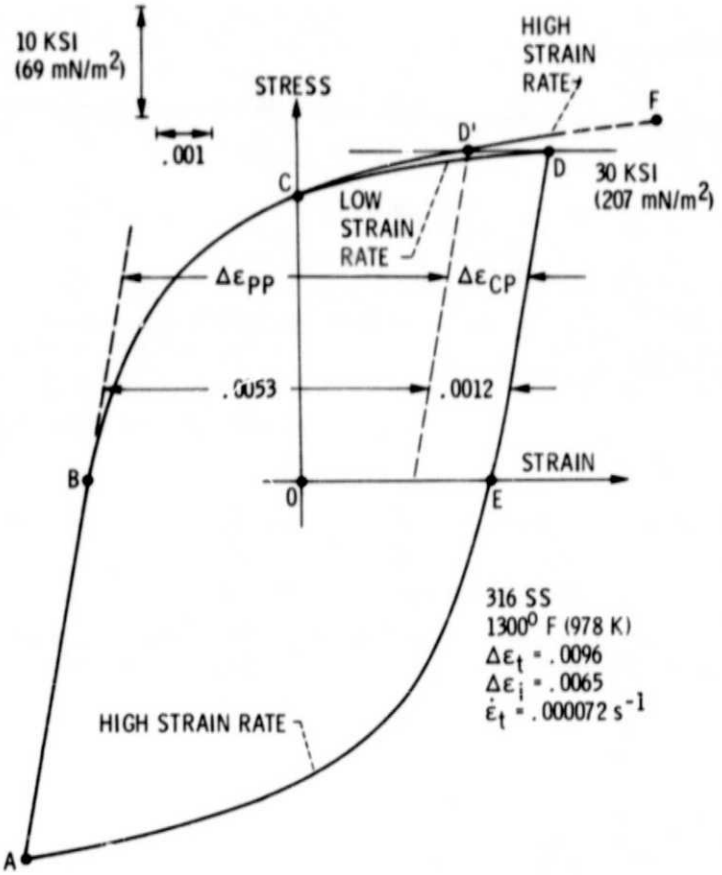

Figure 12. - Illustrative example of partitioning by the half-cycle rapid load-unload method.

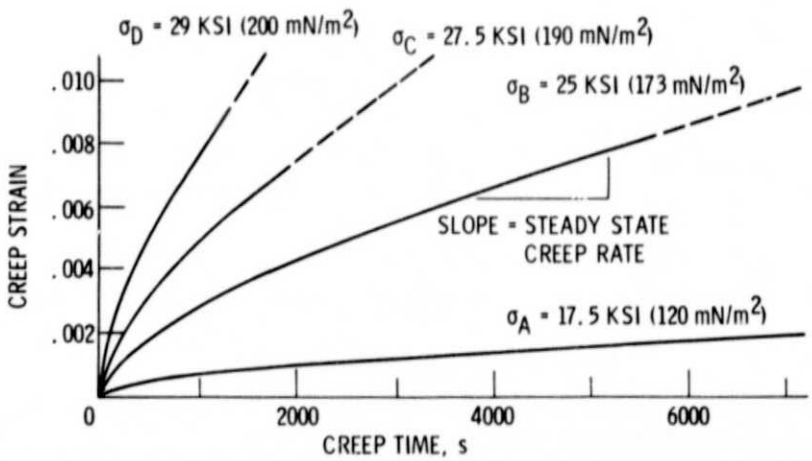

Figure 13. - Creep curves at various points along the stabilized hysteresis loop of Figure 9.

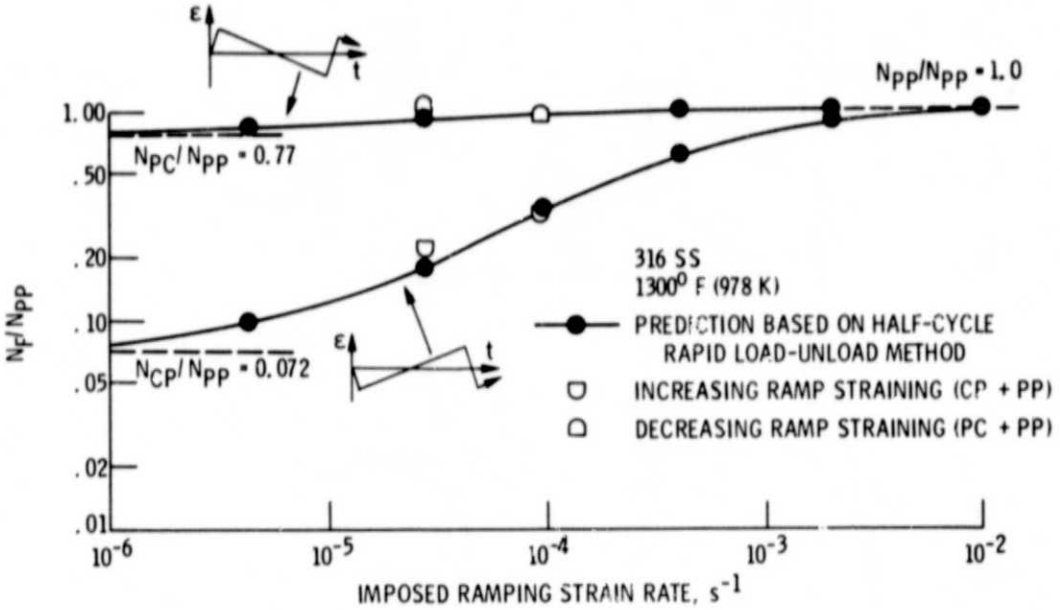

Figure 14. - Comparison of predictions and experimental results for increasing and decreasing ramp straining. Predictions made by the half-cycle rapid load-unload method.

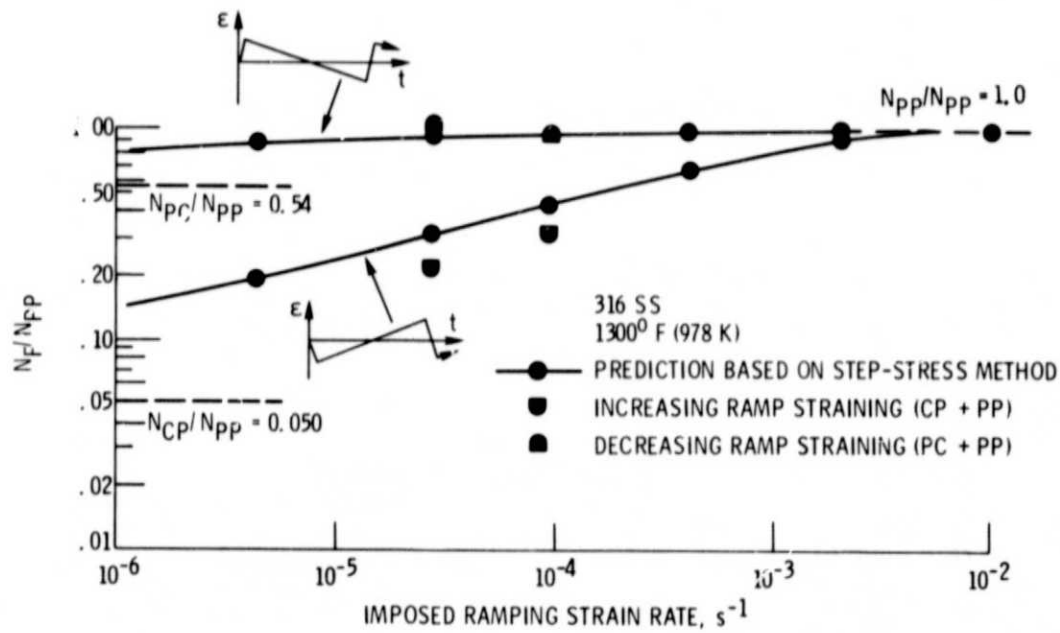

Figure 15. - Comparison of predictions and experimental results for increasing and decreasing ramp straining. Predictions made by the step-stress method.

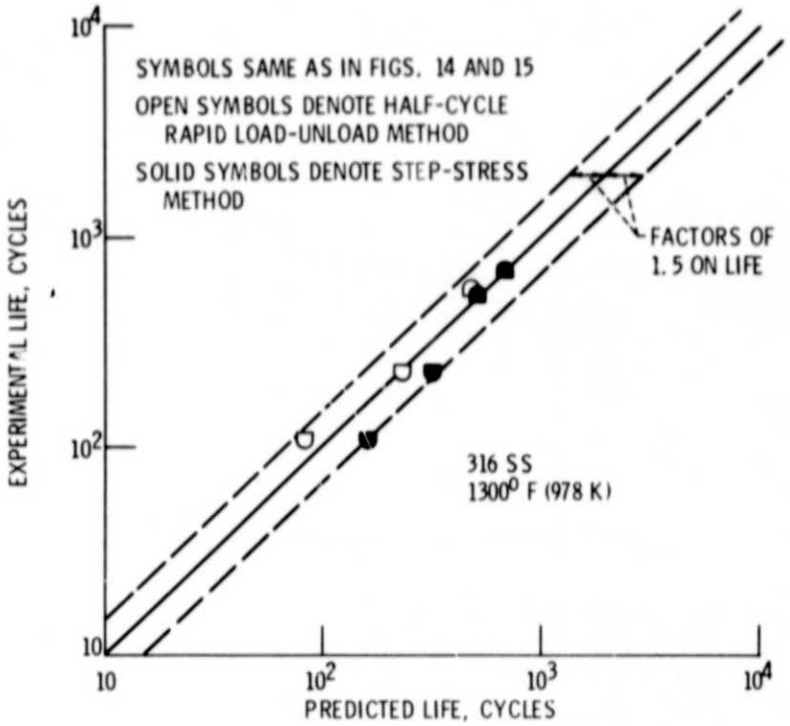

Figure 16. - Predictability of life using two methods of partitioning.

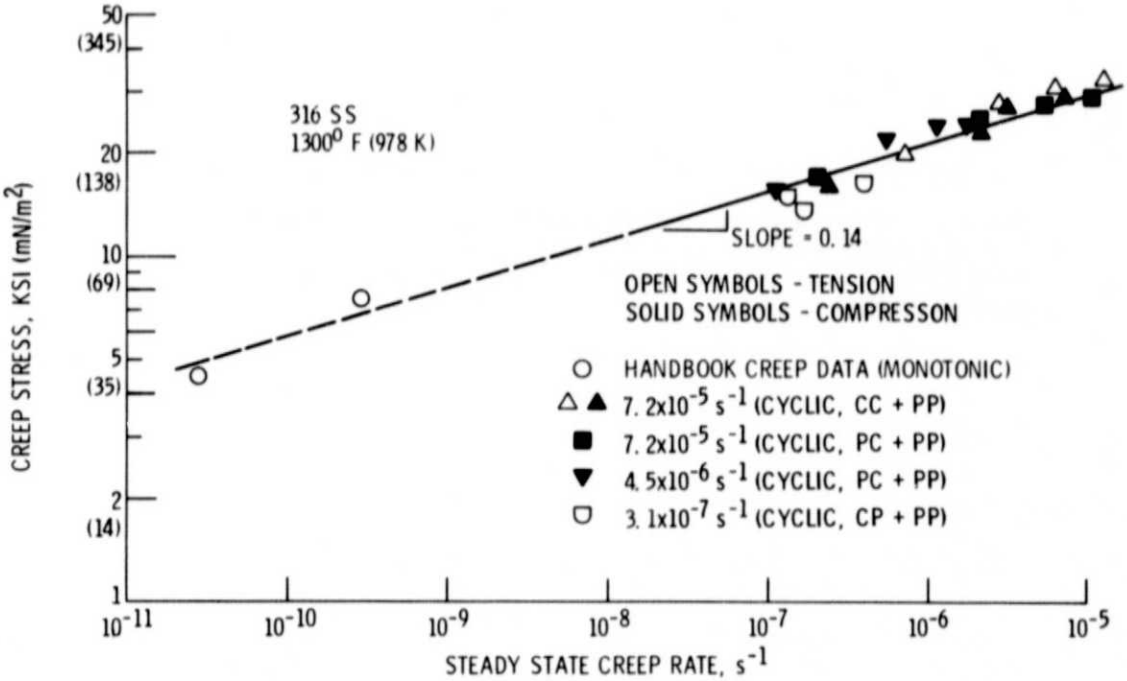

Figure 17. - Correlation of steady state creep rate with stress for a variety of imposed loading histories.

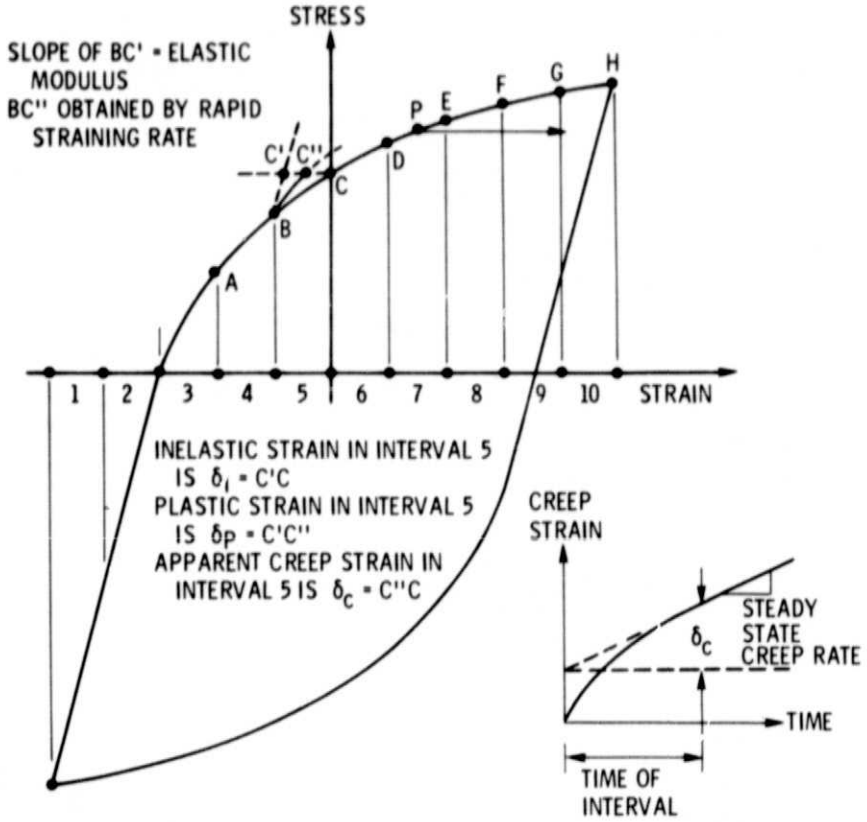

(a) STABILIZED HYSTERESIS LOOP.

(b) CREEP AFTER REACHING POINT P.

Figure 18. - Determination of inelastic strain, plastic strain, and creep strain in each interval of a stabilized hysteresis loop. Illustration for inelastic strain and plastic strain is shown in interval 5 from points B to C; illustration for creep strain is shown in interval 7 at point P.

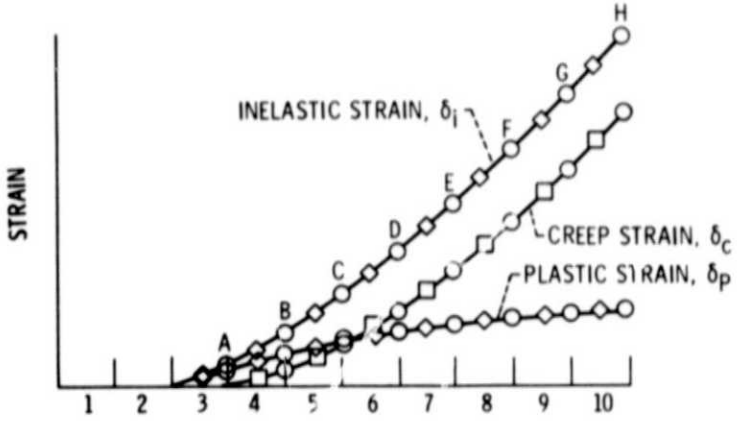

(a) PLOT OF MEASURED COMPONENTS IN EACH INTERVAL.

	PLASTIC	CREEP
BY DIRECT MEASUREMENT	δ_p	δ_c
BY DEDUCTION FROM OTHER MEASUREMENTS	$\delta_i - \delta_c$	$\delta_i - \delta_p$
BY AVERAGING	$\frac{1}{2}(\delta_i + \delta_p - \delta_c)$	$\frac{1}{2}(\delta_i + \delta_c - \delta_p)$

(b) AVERAGING OF DATA.

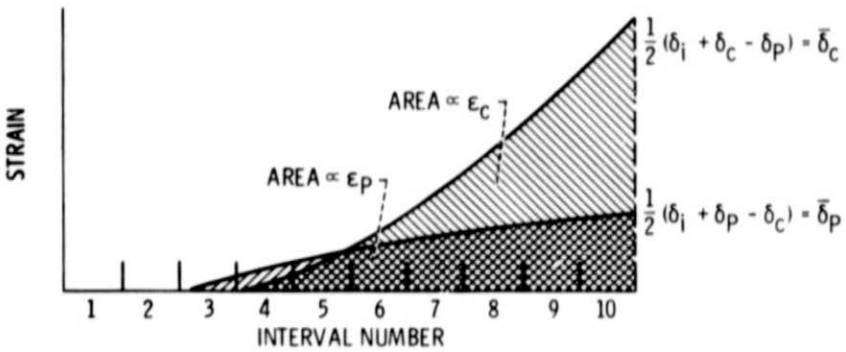

(c) REDUCTION OF DATA.

Figure 19. - Application of measured inelastic strain components in each interval to determine the resultant creep and plastic strains in a half cycle.